

## Climate and Atmosphere Simulator for Experiments on Ecological Systems in Changing Environments

Bruno Verdier,<sup>†</sup> Isabelle Jouanneau,<sup>†</sup> Benoit Simonnet,<sup>‡</sup> Christian Rabin,<sup>‡</sup> Tom J. M. Van Dooren,<sup>§</sup> Nicolas Delpierre,<sup>||</sup> Jean Clobert,<sup>⊥</sup> Luc Abbadie,<sup>§</sup> Régis Ferrière,<sup>#,¶</sup> and Jean-François Le Galliard<sup>\*,†,§</sup>

<sup>†</sup>CNRS/ENS – UMS 3194, CEREEP – Ecotron IleDeFrance, École Normale Supérieure, 78 rue du Château, 77140 St-Pierre-lès-Nemours, France

<sup>‡</sup>Cesbron, Département Recherche et Développement, Rue du Pâtis, Parc d'activités d'Angers, BP 80057, 49181 St-Barthélemy-d'Anjou, France

<sup>§</sup>CNRS/UPMC/ENS – UMR 7618, iEES Paris, Ecole Normale Supérieure, 46 rue d'Ulm, 75005 Paris, France

<sup>||</sup>CNRS/UPS – UMR 8079, Laboratoire Ecologie Systématique et Evolution, Université Paris Sud, Bâtiment 362, 91405 Orsay cedex, France

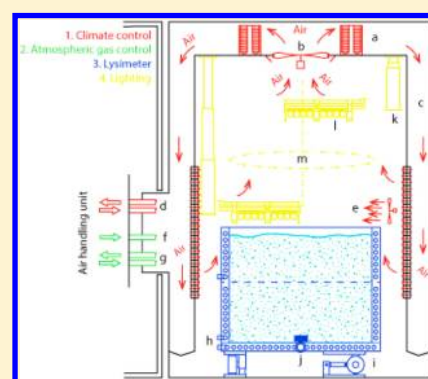
<sup>⊥</sup>Station d'Ecologie Expérimentale du CNRS à Moulis (SEEM), Centre National de la Recherche Scientifique (CNRS), USR 2936, Moulis, 09200 Saint Girons, France

<sup>#</sup>Department of Ecology and Evolutionary Biology, University of Arizona, Tucson, Arizona 85721, United States

<sup>¶</sup>CNRS/ENS - UMR8197 - Institut de biologie de l'Ens, Ecole Normale Supérieure, 46 rue d'Ulm, 75005 Paris, France

### **S** Supporting Information

**ABSTRACT:** Grand challenges in global change research and environmental science raise the need for replicated experiments on ecosystems subjected to controlled changes in multiple environmental factors. We designed and developed the Ecolab as a variable climate and atmosphere simulator for multifactor experimentation on natural or artificial ecosystems. The Ecolab integrates atmosphere conditioning technology optimized for accuracy and reliability. The centerpiece is a highly contained, 13-m<sup>3</sup> chamber to host communities of aquatic and terrestrial species and control climate (temperature, humidity, rainfall, irradiance) and atmosphere conditions (O<sub>2</sub> and CO<sub>2</sub> concentrations). Temperature in the atmosphere and in the water or soil column can be controlled independently of each other. All climatic and atmospheric variables can be programmed to follow dynamical trajectories and simulate gradual as well as step changes. We demonstrate the Ecolab's capacity to simulate a broad range of atmospheric and climatic conditions, their diurnal and seasonal variations, and to support the growth of a model terrestrial plant in two contrasting climate scenarios. The adaptability of the Ecolab design makes it possible to study interactions between variable climate–atmosphere factors and biotic disturbances. Developed as an open-access, multichamber platform, this equipment is available to the international scientific community for exploring interactions and feedbacks between ecological and climate systems.



## ■ INTRODUCTION

To understand the structure and function of ecosystems and predict their responses to environmental change, ecologists must study complex networks of dynamical interactions across multiple temporal and spatial scales.<sup>1–3</sup> To this end, replicated experiments on model ecological systems in microcosms or mesocosms play a critical role.<sup>3,4</sup> Ecological microcosms are miniature constructed ecosystems in which physical and biological conditions are controlled; mesocosms are larger microcosms involving larger and functionally more diverse organisms, and more heterogeneous environments.

Experimental studies of model ecological systems have made major contributions to understanding the fundamental principles of ecology, including organismal plasticity, population dynamics, species coexistence, food-web structure, and

community stability.<sup>4</sup> Mesocosm experiments now also have a key role to play in addressing global change biology, such as ecosystem responses and feedbacks to atmospheric and climate change.<sup>4–6</sup> The lack of mechanistic understanding of ecosystem processes at local scales, and appropriately incorporating this understanding into global models, has been a major source of uncertainties in regional and global predictions.<sup>7</sup> Achieving this mechanistic understanding is precisely the fundamental reason that mesocosm experiments are valuable.<sup>3,8</sup>

**Received:** December 8, 2013

**Revised:** May 11, 2014

**Accepted:** June 23, 2014

**Published:** June 23, 2014

Current challenges in ecosystem sciences call for mesocosm experiments on systems of increasing complexity.<sup>7</sup> Global change research has raised the need not only to assess the impacts of climate change on single species but also to study the dynamics and feedbacks within ecological networks and to acknowledge that biotic interactions and feedback processes lead to complex, nonlinear, and sometimes abrupt responses.<sup>9</sup> The next generation of mesocosm experiments should involve manipulations of multiple factors that are not constant but vary in time and apply differently to different system components.<sup>10</sup> Experimental measurements should encompass multivariate, dynamical responses, and feedbacks on the environment itself.<sup>11</sup> Treatments and measurements should be standardized and replicated across a wide range of ecosystem types.<sup>4</sup> These research objectives are now within reach in principle thanks to recent advances in process-based modeling and data-model assimilation.<sup>12</sup> Formulating alternative hypotheses for the interactions and feedbacks between ecosystem dynamics and environmental change requires integrating direct and indirect effects of the environment on physiological, ecological, and evolutionary processes.<sup>13</sup> Taking advantage of modern statistics, process-based modeling of mesocosm data can embrace such complexity to identify the most important factors and mechanisms.<sup>14</sup> A recent example is the use of process-based models and experimental incubation tests to distinguish among competing hypotheses explaining the short-term response of soil respiration to warming.<sup>15</sup>

With a general modeling framework now firmly in place, the remaining hurdle to next-generation mesocosm experiments has been technological. Previous controlled environmental facilities dedicated to experimental ecosystem research<sup>5,7,16,17</sup> were designed to focus on a single ecosystem type (grassland or freshwater food webs) or to control a small number of climate and atmospheric parameters at constant levels. From 2007 to 2012, we developed and tested the Ecolab system as a variable climate and atmosphere simulator for advanced experimentation on a broad range of ecological systems. The Ecolab specifications aim at the simulation of (i) slow and fast temporal patterns of atmospheric temperature and humidity over ranges that are characteristic of most continental and oceanic surfaces, (ii) temporal patterns of atmospheric gas concentration with great accuracy ( $\text{CO}_2$ ,  $\text{O}_2$ , and  $\text{N}_2$  in the standard specification), and (iii) thermal gradients in the ecosystem's biotope (water or soil) independently of the atmosphere. The technology was optimized to allow the decoupling of environmental factors in an accurate and reproducible manner for the purpose of controlled, replicated experiments. Here, we report the results of performance tests of atmospheric and climatic regulations in the Ecolab prototype and a growth test of a model plant species in two contrasting climate scenarios. Finally, we discuss several research perspectives to which experimentation using the Ecolab simulator could contribute.

## MATERIALS AND METHODS

**General Design.** The Ecolab is a modular and autonomous structure consisting of three walk-in climate chambers, a shared heat and cold production module, the climate–atmosphere distribution modules of each climate chamber, and a laboratory module (Figure 1A and Supporting Information (SI) Table S1). The experimentation modules are made of 100-mm thick polyurethane foam placed on a steel frame and divided in compartments, thus providing excellent thermal insulation. The

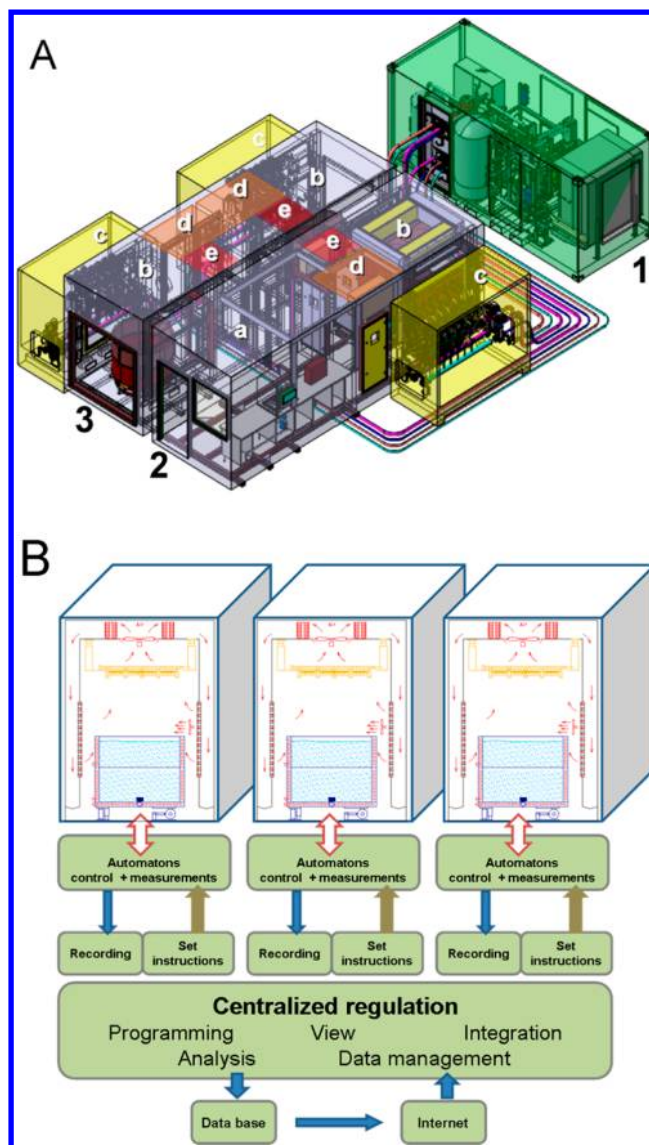


**Figure 1.** Design components of the Ecolab. A. Ground plan of the modular structure including the production module (1) and the two experimentation modules (2, 3). These two experimentation modules share one wet bench space (a) providing access to each climate chamber (b). Environmental conditions inside each climate chamber are independently controlled by a distribution module (c) and the air treatment unit (d). Access to climate chambers is provided through secured airlocks (e). B. Control-command diagram illustrating the main functions of the central supervisor system and some database management tools.

polyester wall surface has a white gel-coat interior finish, which undergoes a long heat treatment to reduce the release of nonpolymerized components and residual volatiles (analysis by GC-MS FET, Cray Valley, France). The chamber volume ( $13 \text{ m}^3$ ) was chosen as a compromise to enable the manipulation of closed, functionally diverse ecological systems while minimizing the response time of controlled variables. A newly developed lysimeter with temperature, weight, and leakage control can be installed inside each chamber to contain a  $1\text{-m}^3$  aquatic or terrestrial ecosystem. This makes it possible to impose thermal conditions independent of the atmospheric temperature. The chamber can accommodate a differential pressure of  $\pm 1000 \text{ Pa}$  during experiments.

The laboratory includes the central supervisor software and system, a wet bench space, and a sealed access to each chamber. Sealed tight locks further allow wiring sensors and samplers from the chambers with computers, instruments, and analyzers located in the laboratory. Each chamber has its own independent set of automation controllers, and environmental conditions inside each chamber are controlled by machines in different functional groups (SI Figure S1). Set-points for environmental conditions are entered into a data file providing instructions to the central supervisor (Omron CX software) by default steps of 5 min. The central supervisor system receives values of state and machine variables every sec and records them every 30 s. Climate and atmosphere conditions of each chamber are piloted by a supervisor that controls the automation system, data visualization, and data recording (Figure 1B). The functional independence of the climate chambers allows replicating experiments across chambers but also staggering them over time.

Each chamber is conditioned by a distribution module and by a technical compartment with the central air conditioning unit for the control of gases and dehumidification (Figure 1A and SI Figure S1). The distribution module is supplied with cold and hot ethylene glycol water from the production module and also hosts a demineralized water production unit supplying rain and air humidity inside the chamber at controlled temperature. The production module contains a heat pump developed specifically for the Ecolab that generates and stores reserves of hot and cold ethylene glycol water into 2 separate tanks, each of approximately 1000 L capacity. We optimized energy consumption by using a tracking system that analyzes the future needs of the chambers and adjusts the temperature of the stored ethylene glycol water in each tank accordingly. The performance coefficient of the heat pump (energy supplied to or removed from the reservoir divided by energy consumed by the heat pump) varies from 1 for a very cold climate to 7 for a warm climate.

The technical compartment includes (i) an adiabatic ultrasonic humidifier (Teddington Vapatronics HU85), (ii) a powerful adsorption dehumidifier filled with silica gel desiccant, (iii) solenoid valves for gas regulation, (iv) a CO<sub>2</sub> absorption system based on soda lime, and (v) the gas analyzers (see SI Table S1 for a list of all sensors). Solenoid valves allow controlling gas concentrations (N<sub>2</sub>, CO<sub>2</sub>, and O<sub>2</sub>) by direct injections and by CO<sub>2</sub> absorption when necessary. This technical compartment is air-conditioned to track temperature changes in the chamber.

**Climate Regulation.** Temperature in the chamber is controlled by a set of four heat exchangers located in a plenum space surrounding the chamber and connected in parallel (2 cold and 2 hot exchangers) to circuits arriving from the production module. Thus, cold and hot ethylene glycol fluids circulate without mixing. The air drawn at a maximum rate of 2.7 m<sup>3</sup>·s<sup>-1</sup> inside the plenum space flows through the heat exchangers where the circulation of cold and hot fluids is controlled by proportional valves. This air is then reintroduced on each side of the chamber and homogenized at a flow of approximately 0.1 m·s<sup>-1</sup> through a honeycomb grid.

When the temperature of the cell is above 1 °C, relative humidity is controlled according to set-points for water weight (or specific humidity) by the combined action of the humidifier and of two modes of dehumidification. When the temperature is below 1 °C, air humidity control is stopped. Reliable measures of very high humidity levels (>97% RH) could not be

obtained with routine probes. The upper limit for humidity in the range 97%–100% RH between 5 and 50 °C was thus verified by measurements with a forced circulation psychrometer. Specific humidity indicates the concentration of water vapor independent of temperature and pressure, whereas relative humidity depends on temperature. The value of relative humidity determines, together with temperature, the water vapor deficit and thus the potential for evapotranspiration. Ultrafine mist (droplets of 1–3 μm) is generated by the piezoelectric ultrasonic humidifier. The air circulates through the humidifier at a controlled rate and moisturized air is reinjected in the chamber. A first dehumidification is performed by the cold ethylene glycol fluid circulating in the heat exchanger at a temperature below the dew point. Water condensate is collected and its quantity can be measured if necessary. During more demanding situations, such as a rise in temperature associated with a set-point at low humidity, dehumidification is ensured by a mobile absorption dehumidifier filled with high-performance desiccant (silica gel). A mechanism installed on the dehumidifier ensures that moist airflow circulates only in one part of the desiccant, while the other part is regenerated in an adjacent compartment at a temperature higher than 105 °C. The water vapor generated in this compartment is condensed locally by a cooling circuit derived from the main circuit of the chamber and condensed water is removed outside of the air treatment unit. Again, this quantity can be measured.

“Rainfall” is defined as an atmospheric input of water in the form of droplets at a controlled size. Rainfall is distributed by sprinklers equipped with programmable proportional valves that allow for different flow rates and droplet sizes. The water used to control air humidity and to produce rainfall is generated by a reverse osmosis system (Teddington L60BP) and then stored in a 100-L stainless steel tank at a controlled temperature above 5 °C. This allows control of water quality and avoids strong thermal contrasts between water and air. Currently, the reverse osmosis unit is supplied with tap water but, in principle, it could be supplied from a tank (e.g., with deuterated water for isotopic labeling) or bypassed to use other sources of water (e.g., ultrapure water). Air movements inside the chamber are of two types: a lateral flow generated by two fans installed on the ceiling and ranging from 0 to 0.5 m·s<sup>-1</sup>, and optional flows provided by three powerful fans that can be attached to the upper part of the lysimeter. These fans are mounted on a stand that allows reorienting them and they produce turbulent flows ranging from 3 to 4 m·s<sup>-1</sup>. Pressure in the chamber is monitored continuously by a differential sensor and secured by an exhaust set at 600 Pa. To absorb changes in chamber pressure caused by climate regulation, a mode of containment at constant pressure and variable temperature is currently under development, modeled after the “lung” of materially closed facilities.<sup>18</sup>

**Atmospheric Gas Regulation.** Atmospheric gas regulation targets N<sub>2</sub>, O<sub>2</sub>, and CO<sub>2</sub>, but can also involve injection of trace gases on demand (for example CH<sub>4</sub> or O<sub>3</sub>). N<sub>2</sub> is supplied by a pure nitrogen generator with high production capacity, O<sub>2</sub> is supplied either from high-pressure bottles or, at a lower cost, through an air inlet deprived of CO<sub>2</sub> (a N<sub>2</sub>–O<sub>2</sub> mixture), and CO<sub>2</sub> is typically supplied from a pure gas bottle. In principle, isotopically labeled CO<sub>2</sub> of different <sup>13</sup>C and <sup>12</sup>C sources may also be injected inside the atmosphere to perform pulse or continuous labeling experiments, but this system is not yet operational and instruments to trace stable C isotopes are not

available on site. CO<sub>2</sub> subtraction is done by absorption during the air circulation inside a separate container equipped with filter plates filled with soda lime. O<sub>2</sub> is subtracted by dilution with nitrogen with simultaneous readjustment of CO<sub>2</sub> content to the set-point. Oxygen levels can be decreased to approximately 4000 ppm. This dilution procedure involves an air outlet in conjunction with nitrogen injection to prevent overpressurization of the chamber. For security reasons, the chamber is locked and access is forbidden under 18% O<sub>2</sub> concentrations.

**Conditioning of Ecosystems and Organisms.** Terrestrial, freshwater, and marine ecosystems can be accommodated in a double-wall stainless steel lysimeter. The lysimeter structure comprises two horizontal belts of 40 cm high each (SI Table S1). The bottom and the two circular belts each have an independent circulation of cold and hot ethylene glycol fluids provided by the distribution module. These three independent regulations allow simulating thermal gradients according to programmed instructions. The lysimeter sits on three strain gauges (Sartorius PR 6241) measuring weight change with  $\pm 300$ -g imprecision at a controlled temperature, equivalent to 0.03% for a 1000 kg ecosystem and lysimeter. Weight measurement depends, however, on thermal stability and must be calibrated. Other equipment is available on demand, such as a temperature-controlled growth tables for plants, microcosms for aquatic communities, or individual tanks for small animal species.

**Artificial Lighting.** The lighting system is set up on a rotating and translating panel that homogenizes light conditions over the ecosystem. A telescopic frame allows adaptation of the distance between the light source and the ecosystem. Air flows through the lighting system at approximately 0.4 m·s<sup>-1</sup> and extracts the heat generated by lighting. A LED-based lighting system has been developed specifically for the Ecolab to program variation in light intensity and spectrum (Jouanneau, unpublished data). Other lighting systems have been successfully tested, such as commercial LED bulbs, plasma lamps, and high-pressure sodium projectors.

**Performance Tests of Climate Regulations.** All climate tests were performed on a prototype in 2011. We measured control accuracy by forcing constant levels of temperatures (from -10 to 40 °C in increments of 10 °C) and humidity (30% RH to 90% by increments of 20%). In general, the relative humidity is not regulated in dry air when the temperature is below 1 °C. However, for the purpose of these tests we attempted humidity regulation at 0 °C. During these simulations, the climate chamber was empty, the CO<sub>2</sub> concentration was set at 450 ppm, and light was provided by our LED system. Each combination of temperature and relative humidity was simulated for a period of several hours (SI Appendix S1 Figure S2).

In addition, we simulated a sequence of five variable climate types including a cold climate with temperatures below -5 °C (Kevol, Finland), a temperate climate (Foljuif, France), a hot and dry desert climate (Adrar dry, Algeria), the same desert climate in the presence of an aquatic ecosystem (lysimeter filled with freshwater, Adrar wet), and a humid tropical climate (Ahmedabad, India). We repeated the simulations of Kevo, Foljuif, Adrar wet, and Ahmedabad twice in the same chamber with an interval of one month between repeats. Following ISO 5725, we estimated bias (mean difference between the measured value and the set-point, also called trueness) and imprecision (sampling standard deviation), and we calculated

accuracy as the square root of the mean square error (MSE), where  $MSE = bias^2 + precision^2$ . High values for bias, imprecision, and square root of MSE indicate inaccurate control relative to the set-point.

**Performance Tests of CO<sub>2</sub> Regulation.** Five stable levels of atmospheric CO<sub>2</sub> representative of pre- and postindustrial levels observed in nature were simulated in fluctuating climates. These tests were conducted in the prototype chamber with enhanced equipment compared to the basic level of equipment used for climate tests. We analyzed the data in the same way as previously.

**Thermal Gradient Regulation in the Lysimeter.** We tested the quality of the thermal gradient control of the lysimeter with an aquatic habitat (freshwater) under constant levels of temperature in the air and in each belt of the lysimeter. Temperature in the aquatic habitat was measured every 30 s at eight depths in a 75-cm water column and at the water surface using Pt100 probes placed in the center of the lysimeter. To simulate a thermal gradient similar to that of some shallow lakes during the summer days in temperate zones,<sup>19</sup> we started with three different temperature set-points in the lysimeter (bottom 15 °C, lower belt 20 °C, upper belt 25 °C) and the same temperature in the air as in the surface water (25 °C). We then mimicked a temperature increase of 4 °C similar to the one used in several warming experiments with freshwater ecosystems.<sup>6</sup> This was done by increasing step-by-step the temperature set-points in the air, in the upper belt, in the lower belt, and in the bottom of the lysimeter. We also increased temperature set-points only in the lower belt and only in the bottom of the lysimeter to simulate warming at the bottom of the water column independently from surface conditions. Each simulation lasted for 12 h to allow the calculation of the water thermal gradient at equilibrium.

**Biological Test.** We ran one biological test to examine growth pattern and thermal sensitivity of one model terrestrial plant. How the physiological response of organisms to a short-term, large-amplitude temperature increase will constrain or facilitate their acclimation or adaptation to long-term gradual changes is indeed an important open question.<sup>9</sup> Here, we assessed the effects of increased air temperature on the seasonality of leaf biochemical and functional properties (i.e., photosynthetic capacity) in sessile oak trees (*Quercus petraea* Liebl 1784) during a 5-month simulation from early summer conditions to the autumn alteration of leaf functional properties. There is growing evidence that higher summer temperature delays the occurrence of leaf senescence and fall in temperate trees.<sup>20</sup> However, we still know little about climate effects on nitrogen resorption from leaves and on reduced nitrogen investment in the photosynthetic apparatus, two core processes that lead to reduced leaf photosynthetic capacity in autumn. Two populations of 36 1-year-old seedlings were placed in two chambers under contrasting temperature regimes from the end of July (i.e., after reaching leaf maturity) until complete senescence. Both temperature regimes were constructed to follow the weather seasonal pattern of the study region (80 km SE of Paris, with +10.9 °C annual average), increased or reduced by 3 °C, respectively for the “warm” and the “cold” treatments. In both treatments, the photoperiod was varied daily to follow the local conditions, with light provided by Hydrargyrum quartz iodide projectors (average light flux = 400  $\mu\text{mol PAR m}^{-2}\cdot\text{s}^{-1}$ ). The atmospheric humidity was set to 1 kPa vapor pressure deficit, and soil moisture was maintained above the water-stress threshold through regular watering.

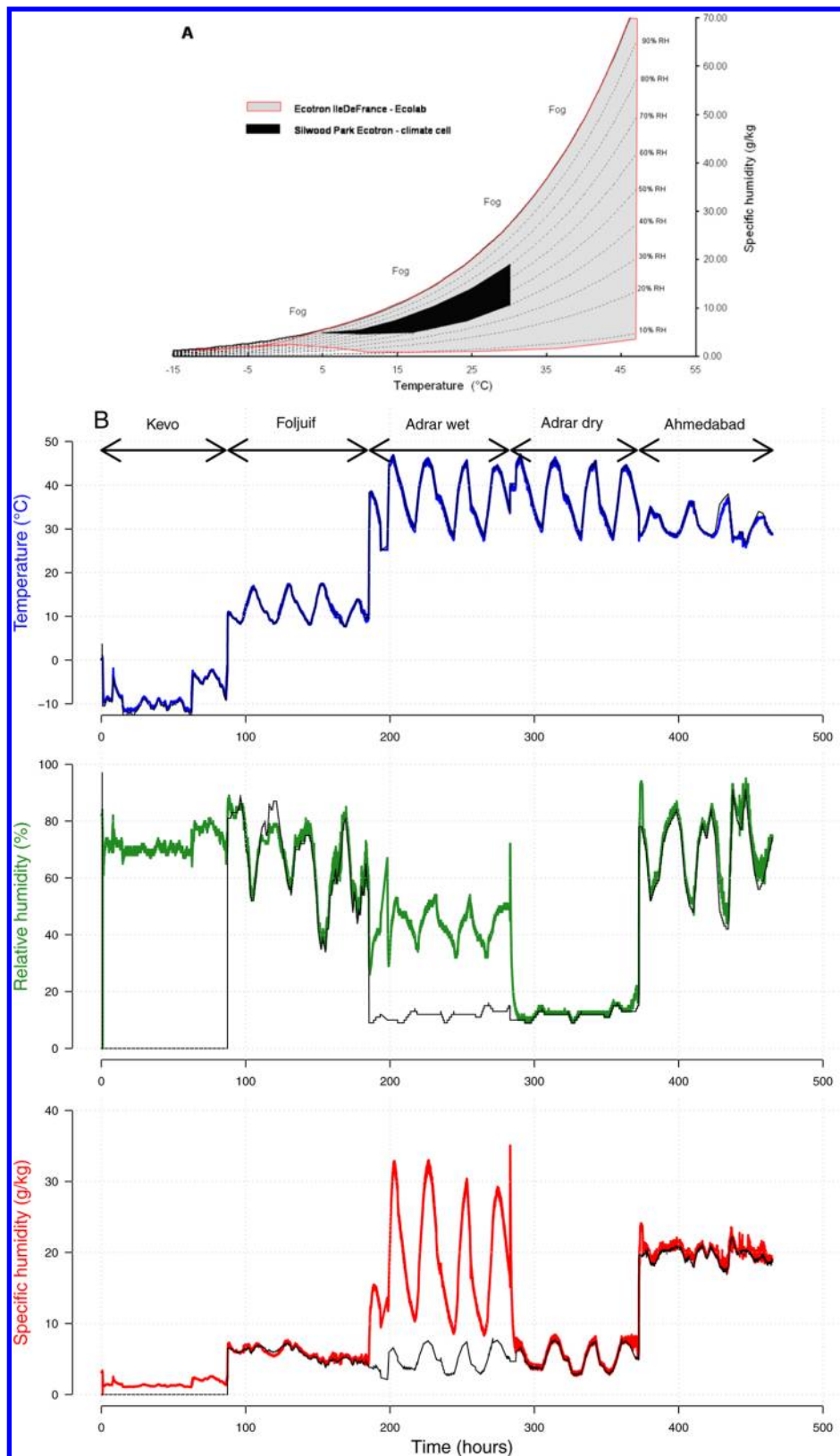


**Figure 2.** Climate performances. (A) Psychrometric chart at the atmospheric pressure (1013 hPa). Limits were tested by imposing a maximal dehumidification set-point from 0 to 45 °C, a humidification sequence at 47 °C, and a maximal humidification from 47 to –13 °C. Performance of the Ecotron Silwood Park is presented for comparison after data reported in ref 16. (B) Daily fluctuations of temperature (°C) and humidity (relative and specific values) for a sequence of five experimental conditions: 1. Climate in Kevo, Finland. 2. Climate in Saint-Pierre-lès-Nemours, France. 3. Climate in Adrar, Algeria in the presence of an aquatic environment. 4. Climate in Adrar, Algeria without the aquatic environment. 5. Climate in Ahmedabad, India. Sequences of set-points (black curves) were constructed from meteorological data converted to set points with 5-min intervals (<http://www.meteociel.fr/climatologie/climato.php>). Data (colored curves) were collected every 30 s.

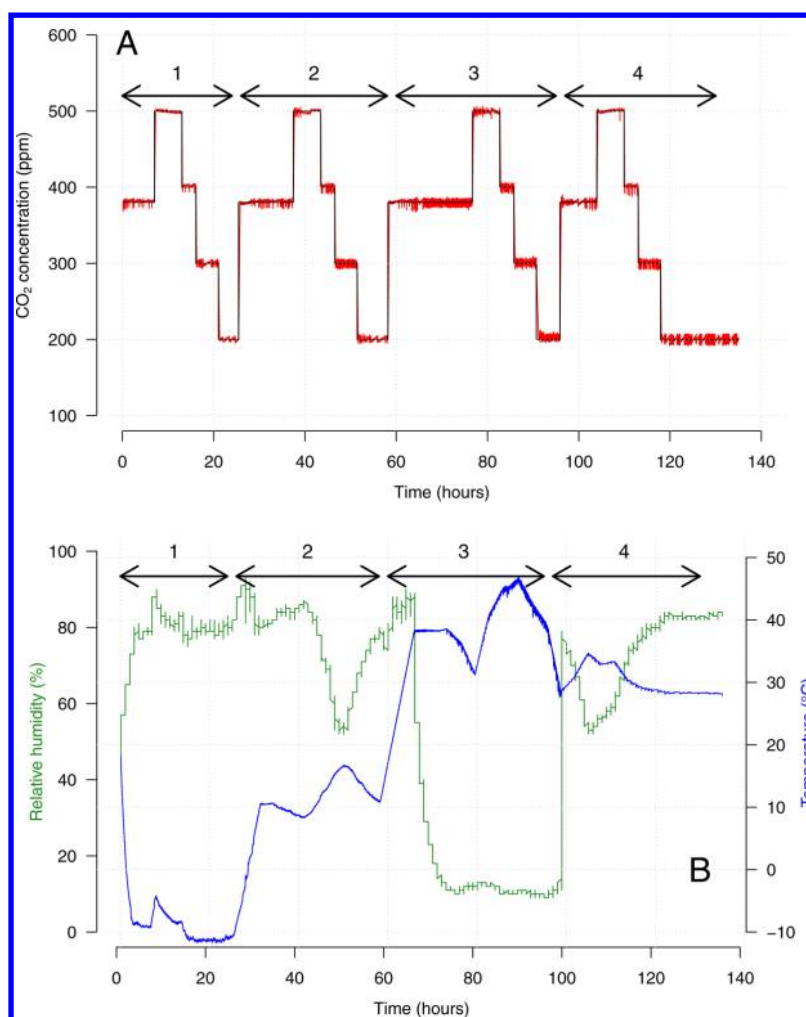


**Figure 3.** Efficiency of control of atmospheric CO<sub>2</sub> concentration (A), depending on climate conditions (B). (A) Measurements (red curve) and set-points (black curve) for set-points (black curve) at 380, 500, 400, 300, and 200 ppm. (B) Tests are repeated in four variable weather conditions: cold (1), temperate (2), hot and dry (3), and hot and humid weather (4).

Throughout the experiment, we surveyed several structural, biochemical, and functional properties of a subset of 10–15 leaves per treatment on a weekly basis. The leaf chlorophyll content was measured optically with a Dualex-4 device (FORCE-A, Orsay, France). Leaf chlorophyll content was averaged over 8 optical measurements taken on the ad- and abaxial faces of the leaf. The leaf photosynthetic maximum activity was measured with a LI-6400 device (Licor, Lincoln, NE USA) at saturating light (PPFD = 1000  $\mu\text{mol m}^{-2}\cdot\text{s}^{-1}$ ) under ambient CO<sub>2</sub> concentration (400 ppm) and controlled atmospheric humidity (1 kPa).

## RESULTS

**Technological Advances.** The goals of climate and atmosphere regulation across a large spectrum of environmental conditions, of integration of these regulations into a centralized program, and of energetic efficiency, raised serious technical challenges. The modular design with one heat pump per Ecolab rather than a single, large production unit was chosen to improve control at thermal extremes, and also to ensure greater resilience of experimental design to heat pump failure. Production and storage by this powerful air–air heat pump was also optimized. The broad spectrum of environmental conditions was achieved thanks to the complete

separation of hydraulic and airflow networks and to the integration of the air conditioning system into the modular structure. This enabled parallel injection of several gases and CO<sub>2</sub> absorption and a thermal preconditioning of all secondary air circuits to avoid condensation.

**Maximal Performances.** The psychrometric chart (Figure 2A) shows the combinations of temperature and relative humidity (RH) that can be realized at a given pressure. Air temperature can vary from  $-13$  to  $47$  °C at a maximum speed of  $0.6$  °C·mn<sup>-1</sup> and from  $47$  to  $-13$  °C at a maximum speed of  $-0.17$  °C·mn<sup>-1</sup>. The lower limit for humidity around 7% was reached by gradually increasing the temperature set-point from the lowest temperature ( $-13$  °C) after programming the lowest humidity (0%). The upper limit for humidity was obtained by tracking the dew point stepwise during a slow descent of the temperature from  $47$  °C at 97% HR to  $-13$  °C. The humidification system can produce an increase of about 7 g H<sub>2</sub>O per kg dry air per minute. At high temperature, the airflow results in significant condensation on the cold heat exchanger and a net balance of water production of approximately 1.75 g H<sub>2</sub>O per kg dry air per minute, which makes it possible to increase relative humidity from 7% to 97% (fog) at  $47$  °C in approximately 1 h. This humidification capacity increases at lower temperatures. Dehumidification power at  $25$  °C allows

varying humidity from 20 (99% RH) to 1.36 g per kg dry air (7% RH) with a speed of about 0.03 g per kg of dry air per minute. This performance diminishes with the evaporation of the ecosystem.

**Climate Simulations.** We illustrate the performance and limitations of the Ecolab by simulating 20 contrasted levels of temperature and humidity (SI Appendix S1 Figure S2) and by replicating (two series) five real climates during 4 days (Figure 2B). During the first tests, accuracy is high and equals on average  $\pm 0.26$  °C for temperature and  $\pm 2.7\%$  for relative humidity. Regulated humidity is less accurate when the humidity set-point increases and the air is colder (SI Table S2). During the second tests, the Ecolab faithfully reproduces the daily dynamics of the four model climates except for some discrepancies: humidity is not regulated at a temperature below 1 °C, and some humidity levels cannot be achieved in the desert climate in the presence of large volume of water (see SI Appendix S1 Table S3). The two independent repetitions of the climate simulations are virtually indistinguishable, thus indicating very good repeatability (SI Figure S3 and Table S4). Additional tests and the quantification of bias, imprecision, and repeatability are provided as additional information (SI Appendix S1).

**Atmospheric Gas Regulation.** Controlled CO<sub>2</sub> is very accurate in constant climate conditions but also when temperature and humidity conditions are variable (Figure 3). Irrespective of the tested climate, set-points for CO<sub>2</sub> concentration are closely matched (bias and accuracy around 3 ppm). The increase of CO<sub>2</sub> is about 7 ppm per minute depending on CO<sub>2</sub> injection flow, while the maximum absorption capacity of the fresh soda lime system is about 30 ppm per minute. Further quantitative analyses are given in SI Appendix S2. In addition, control of O<sub>2</sub> is performed with an imprecision of  $\pm 200$  ppm, equivalent to 1% of the mean O<sub>2</sub> concentration (results not shown). The depletion of oxygen is obtained in a few hours depending on the flow of continuous injection of nitrogen. A level of extreme hypoxia of 450 Pa (about 4000 ppm or 0.4% by volume) is obtained in 10 h by injecting pure nitrogen. Thus, the partial pressures of oxygen and carbon dioxide observed contemporarily at high altitudes can be simulated. For example, to simulate physiological gas exchange conditions at an altitude of 4000 m (Pa = 617 hPa) when the Ecolab is located at sea-level atmospheric pressure, conditions inside the chamber can be set to 129 hPa pO<sub>2</sub> (i.e., 12.8% O<sub>2</sub>) and a pCO<sub>2</sub> of 23.4 Pa (i.e., 0.023% CO<sub>2</sub>).

**Thermal Regulation of the Lysimeter.** When the lysimeter is filled with water, thermal regulation allows simulation of a stable temperature difference between the bottom and the surface of the water column, including a steep thermal gradient typical of lakes that show a warm water body at the surface (called epilimnion) and a cold water body beneath (called hypolimnion, see SI Appendix S3). This thermal stratification has a decisive impact on ecological processes and geochemical cycles.<sup>19</sup> A temperature increase of +4 °C can be imposed on each component of the water column, making it possible to analyze additive and interactive effects of warming on surface, water, and sediment layers (SI Appendix S3). In addition, by decreasing surface temperatures, it is possible to mix water layers and simulate cycles of thermal stratification and gradient removal typical of lakes (results not shown, see ref 19). Other set-point rules can easily be programmed and soil thermal gradients can also be emulated.

The thermal stratification of the soil will depend on its thermal conductivity, its biological activity, and the surrounding climate.

**Biological Test.** Our populations of trees developed normally and showed realistic seasonal dynamics for both leaf chlorophyll content and maximum photosynthetic capacity (Figure 4). In addition, the experiment validates the hypothesis

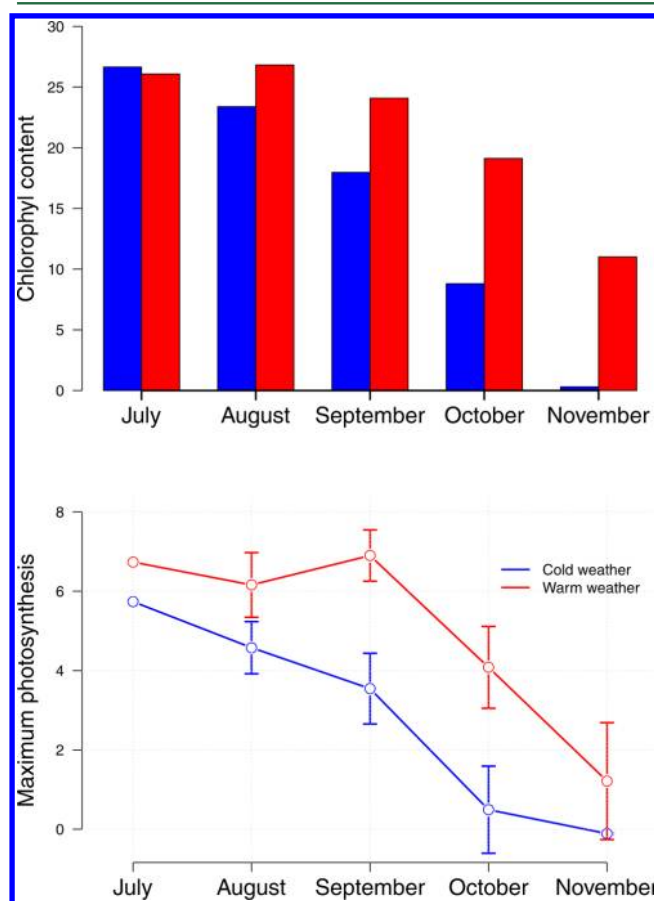


**Figure 4.** Effects of variable weather conditions across a vegetative growth season in a tree species. Seasonal dynamics of leaf chlorophyll content ( $\mu\text{g}\cdot\text{cm}^{-2}$ ) and maximum photosynthetic activity ( $A_{\text{max}}$ ,  $\mu\text{mol}\cdot\text{m}^{-2}\cdot\text{s}^{-1}$ ) were recorded in sessile Oak. Oak trees were raised during simulation of two weather dynamics with constant contrast in temperature and the same water vapor deficit (1 kPa) obtained by adjusting the relative humidity in each chamber.

of an acceleration of biochemical and functional senescence of leaves caused by cold temperature. Complementary analyses are underway to quantify the seasonal activity of Rubisco (the core photosynthetic enzyme) and assess the relative influences of the loss of pigmentation and reduction of enzyme activity in the temperature-driven seasonality of photosynthesis.

## DISCUSSION

The responses of ecological systems to climatic and atmospheric changes are mediated by complex networks of biotic interactions. To improve our mechanistic understanding of the resulting indirect effects and feedbacks<sup>9</sup> and the management of ecological systems,<sup>21</sup> we need multifactor, multivariate experimental data that can be combined with process-based models. The Ecolab simulator is a novel research instrument designed toward this goal and is now available to the international scientific community through calls for projects

(www.ir-ecotrons.cnrs.fr). Our biological test demonstrates the feasibility of short-term experiments over a few months involving the simulation of environmental variation experienced by individual organisms during their lifetime. The study of photosynthetic variation in temperate deciduous trees was motivated by how directional change in climate will alter seasonal ecosystem processes such as leaf senescence, a life history switch that involves reallocation of nutrients by the organism in response to climate and atmosphere variation.<sup>22</sup> Since this biological test, the Ecolab has hosted projects that involve environmental genomics with the model plant *Arabidopsis thaliana*, animal metabolism, life history decisions of hatching in annual fishes, photosynthesis in crop plants, and carbon dynamics in freshwater communities. Hereafter, we further discuss the scope of the Ecolab facility for future ecosystem experimental research.

**Spatial and Temporal Scale of Experimentation.** The Ecolab chamber volume (13 m<sup>3</sup>) compares to the NERC Ecotron chambers<sup>16</sup> and enables the manipulation of closed, functionally diverse ecological systems from a few days to several months while minimizing the response time of controlled environmental variables and limiting dilution of experimental effects. By simulating climate scenarios predicted for the future or observed in the past, the Ecolab will make it possible to examine short-term responses to steep changes in environmental conditions, including changes in mean temperature or frequency of rainfall events for example. Thus, as in other global change experiments facilities,<sup>23,24</sup> complex feedbacks occurring at large spatial and temporal scales as a consequence of slow gradual climate changes will be beyond the scope of this equipment. Yet, by focusing on communities of small organisms with short generation time, the Ecolab volume should allow probing important ecological and evolutionary processes.<sup>8</sup> In particular, the Ecolab can host the “uncultured majority” of bacteria and protista that play key roles as recipients and agents of global climate change and thus may help “open the microbial blackbox” of ecosystem models.<sup>2,25</sup> Critical questions include to what extent global change drives adaptation in microbes, and how adaptive dynamics in microbes interact to alter community composition and ecosystem function. These questions are especially pressing for marine ecosystems, in which microorganisms are major agents of biogeochemical fluxes.<sup>26</sup> In addition, processes that occur over large spatial scales (such as long-distance dispersal) and long time scales may be emulated by manual introductions and by using different initial conditions in different treatments, respectively.<sup>8,27</sup> Such data could be integrated with process-based models to “scale up” mesocosm dynamics and handle potential side effects introduced by the containing walls (e.g., ref 28).

**Range of Climate and Atmosphere Variation.** Different ecological systems may respond differently to climate change and may be sensitive to different climate factors.<sup>29</sup> It is therefore important that the range of study organisms and ecosystems be as wide as possible. The Ecolab performance tests demonstrate accurate control of atmospheric temperature ( $\pm 0.2$  °C), relative humidity ( $\pm 3$ –5% RH), and CO<sub>2</sub> concentration ( $\pm 3$ –5 ppm) over broad ranges. The Ecolab can faithfully simulate daily and seasonal fluctuations in climate recorded across a wide range of latitude, altitude, or biome types. The injection–absorption system is highly reactive and allows maintenance of constant pCO<sub>2</sub> in variable climates or simulation of variations in pCO<sub>2</sub> in a constant climate. High

repeatability scores show that experiments can be repeated in time and between chamber, a critical feature for experimental design and statistical inference from replicated studies. Other parameters not shown here can also be regulated with high precision, including duration and intensity of lighting, atmospheric concentrations of O<sub>2</sub>, and quantity and quality of the water supply by rainfall. Limits on the Ecolab performance were indicated by simulating unusual conditions, such as a wet biotope in a dry climate. Climate manipulation experiments typically assume that the ecological processes under consideration are at or near equilibrium state and miss variation over multiple temporal scales (diurnal, seasonal, long-term directional) and contrasted ranges.<sup>24</sup> In contrast, the Ecolab allows studying the speed or time lag with which different abiotic and biotic variables respond to different patterns and rates of environmental change. This will help predict threshold effects and ecosystem “catastrophic” tipping points,<sup>11</sup> and address the lack of knowledge on how extreme climatic events affect biodiversity and ecosystem processes.<sup>10</sup> Examples of relevant simulations for future climate change experiments on soil–plant communities may include changes in the timing of frost events, in the intensity of rainfall events, or in the duration of a summer drought.

**Multifactorial Control.** Concurrent changes in multiple factors potentially trigger complex interactive influences on ecosystem structure and function,<sup>30</sup> but a limited experimental capability has been available thus far to evaluate the importance of these interactive effects. The Ecolab permits the simultaneous manipulation of multiple atmospheric parameters together with climatic variables and ecosystem types, which represents a significant advance over other controlled environmental facilities and field experiments.<sup>5,7,16</sup> Potential applications include the study of the interactions between climate warming and water stress, between warming and increased atmospheric CO<sub>2</sub>, between warming and acidification of surface waters, and between environmental change and biodiversity loss. For example, new experiments in the Ecolab could unravel the eco-evolutionary responses of phytoplankton communities to multiple simultaneously changing critical environmental factors, such as elevated CO<sub>2</sub>, UV light, and temperature.<sup>31</sup> The Ecolab is also well suited to address local ecological processes that operate at the interface between different media, such as water and sediments or soil and atmosphere. The ability to perform experiments in which the biotope temperature is controlled independently of the atmosphere is one distinctive feature demonstrated here by simulations of thermal gradients in a shallow water column. The thermal gradient of a soil or water column affects a variety of fundamental ecological processes such as root respiration, soil microbial decomposition, or the vertical distribution of species (e.g., refs 19 and 32). Decoupling variation of temperature between different ecosystem components will help answer high-priority research questions, such as how climate, soil properties, and biotic factors interact to influence soil carbon cycling and nitrogen fluxes across different types of ecosystems.<sup>6,33,34</sup> In addition, the understanding of effects of warming on the ecology and geochemistry of surface, water, and sediment layers will be facilitated.<sup>19</sup>

## CONCLUSION

There is consensus in the scientific community<sup>4,11</sup> on the need for multifactor experiments with (1) explicit inclusion of biodiversity in a broad range of ecosystem types, (2) control of

timing and intensity of global change factors, and (3) evaluation of multivariate nonlinear responses and assessing feedbacks on environmental drivers. The Ecolab simulator facilitates experiments satisfying these requirements. Developed as a large, multichamber platform, the Ecolab simulator will be available to the international scientific community for controlled, replicated experimentation on ecosystem–climate interactions. A grid of six Ecolab simulators (18 chambers) is currently under construction. The first cluster of ten chambers is open to users. Projects are selected among responses to competitive, externally peer-reviewed calls for projects (<http://www.irceotrons.cnrs.fr/>).

## ■ ASSOCIATED CONTENT

### 🔗 Supporting Information

Table S1: Technical specifications of the Ecolab. Figure S1: Functional groups of equipment of the Ecolab. Appendix S1: Accuracy of climate regulation. Appendix S2: Accuracy of CO<sub>2</sub> regulation. Appendix S3: Regulation of thermal gradient. This material is available free of charge via the Internet at <http://pubs.acs.org>.

## ■ AUTHOR INFORMATION

### Corresponding Author

\*Phone: 01.64.28.12.00; fax: 01.64.28.62.06; e-mail: [cereep@biologie.ens.fr](mailto:cereep@biologie.ens.fr)

### Notes

The authors declare no competing financial interest.

## ■ ACKNOWLEDGMENTS

We thank three anonymous reviewers for comments that helped improve a previous version of this manuscript. The Ecolab was developed by a working group of experts from the Ecology-Evolution, BIOEMCO, and Ecology-Systematics-Evolution CNRS units supported by CNRS, Ecole Normale Supérieure, and the Conseil régional d'Ile-de-France. The prototype was funded by grants from CNRS, DDRT (2004-15), ANR (ANR-2005-CPER IDF-134), and Conseil régional d'Ile-de-France (IF-05-099/R). Ecotron IleDeFrance is supported by the Research Infrastructures program Ecotrons from the CNRS and the French research infrastructure AnaEE-Services (ANR-11-INBS-0001). We thank Beatriz Decencièrre Ferrandièrre, Gérard Lacroix, Thomas Tully, Jean-Marc Guarini, Françoise Gaill, and Yvan Lagadeuc for their support. Equipment mentioned in this article is protected in Europe by patents EP2180038 (Ecolab system), EP2180039 (lysimeter), and EP09306076 (LED lighting), and can be purchased at [www.cesbron.com](http://www.cesbron.com).

## ■ REFERENCES

- (1) Loreau, M. *From Populations to Ecosystems: Theoretical Foundations for a New Ecological Synthesis*; Princeton University Press: Princeton, NJ, USA, 2010; p 297.
- (2) Pomati, F.; Jokela, J.; Simona, M.; Veronesi, M.; Ibelings, B. W. An automated platform for phytoplankton ecology and aquatic ecosystem monitoring. *Environ. Sci. Technol.* **2011**, *45* (22), 9658–9665.
- (3) Jessup, C. M.; Kassen, R.; Forde, S. E.; Kerr, B.; Buckling, A.; Rainey, P. B.; Bohannan, B. J. M. Big questions, small worlds: Microbial model systems in ecology. *Trends Ecol. Evol.* **2004**, *19* (4), 189–197.

- (4) Benton, T. G.; Solan, M.; Travis, J. M. J.; Sait, S. M. Microcosm experiments can inform global ecological problems. *Trends Ecol. Evol.* **2007**, *22* (10), 516–521.

- (5) Arnone, J. A.; Verburg, P. S. J.; Johnson, D. W.; Larsen, J. D.; Jasoni, R. L.; Lucchesi, A. J.; Batts, C. M.; von Nagy, C.; Coulombe, W. G.; Schorran, D. E.; Buck, P. E.; Braswell, B. H.; Coleman, J. S.; Sherry, R. A.; Wallace, L. L.; Luo, Y. Q.; Schimel, D. S. Prolonged suppression of ecosystem carbon dioxide uptake after an anomalously warm year. *Nature* **2008**, *455* (7211), 383–386.

- (6) Yvon-Durocher, G.; Jones, J. L.; Trimmer, M.; Woodward, G.; Montoya, J. M. Warming alters the metabolic balance of ecosystems. *Proc. R. Soc. London, Ser. B* **2010**, *365* (1549), 2117–2126.

- (7) Osmond, B.; Anyan, G.; Berry, J.; Langdon, C.; Kolber, Z.; Lin, G. H.; Monson, R.; Nichol, C.; Rascher, U.; Schurr, U.; Smith, S.; Yakir, D. Changing the way we think about global change research: Scaling up in experimental ecosystem science. *Global Change Biol.* **2004**, *10* (4), 393–407.

- (8) Drake, J. M.; Kramer, A. M. Mechanistic analogy: How microcosms explain nature. *Theor. Ecol.* **2012**, *5* (3), 433–444.

- (9) Walther, G. R. Community and ecosystem responses to recent climate change. *Philos. Trans. R. Soc., B* **2010**, *365* (1549), 2019–2024.

- (10) Jentsch, A.; Kreyling, J.; Beierkuhnlein, C. A new generation of climate-change experiments: Events, not trends. *Front. Ecol. Environ.* **2007**, *5* (7), 365–374.

- (11) Rustad, L. E. The response of terrestrial ecosystems to global climate change: Towards an integrated approach. *Sci. Total Environ.* **2008**, *404* (2–3), 222–235.

- (12) Clark, J. S. Why environmental scientists are becoming Bayesians? *Ecol. Lett.* **2005**, *8* (1), 2–14.

- (13) O'Connor, M. I.; Selig, E. R.; Pinsky, M. L.; Altermatt, F. Toward a conceptual synthesis for climate change responses. *Global Ecol. Biogeogr.* **2012**, *21* (7), 693–703.

- (14) Ogle, K. Hierarchical Bayesian statistics: Merging experimental and modeling approaches in ecology. *Ecol. Appl.* **2009**, *19* (3), 577–581.

- (15) Tucker, C. L.; Bell, J.; Pendall, E.; Ogle, K. Does declining carbon-use efficiency explain thermal acclimation of soil respiration with warming? *Global Change Biol.* **2013**, *19* (1), 252–263.

- (16) Lawton, J. H.; Naeem, S.; Woodfin, R. M.; Brown, V. K.; Gange, A.; Godfray, H. J. C.; Heads, P. A.; Lawler, S.; Magda, D.; Thomas, C. D.; Thompson, L. J.; Young, S. The Ecotron - A controlled environmental facility for the investigation of population and ecosystem processes. *Philos. Trans. R. Soc. London, B* **1993**, *341* (1296), 181–194.

- (17) Verschoor, A. M.; Takken, J.; Massieux, B.; Vijverberg, J. The Limnotrons: A facility for experimental community and food web research. *Hydrobiologia* **2003**, *491* (1–3), 357–377.

- (18) Walter, A.; Carmen Lambrecht, S. Biosphere 2 Center as a unique tool for environmental studies. *J. Environ. Monit.* **2004**, *6* (4), 267–277.

- (19) Boehrer, B.; Schultze, M. Stratification of lakes. *Rev. Geophys.* **2008**, *46* (2), 1–27.

- (20) Delpierre, N.; Dufirène, E.; Soudani, K.; Ulrich, E.; Cecchini, S.; Boé, J.; François, C. Modelling interannual and spatial variability of leaf senescence for three deciduous tree species in France. *Agric. Forest Meteorol.* **2009**, *149*, 938–948.

- (21) Arrow, K.; Daily, G.; Dasgupta, P.; Levin, S.; Mäler, K.-G.; Maskin, E.; Starrett, D.; Sterner, T.; Tietenberg, T. Managing ecosystem resources. *Environ. Sci. Technol.* **2000**, *34* (8), 1401–1406.

- (22) Polgar, C. A.; Primack, R. B. Leaf-out phenology of temperate woody plants: From trees to ecosystems. *New Phytol.* **2011**, *191* (4), 926–941.

- (23) Stewart, R. I. A.; Dossena, M.; Bohan, D. A.; Jeppesen, E.; Kordas, R. L.; Ledger, M. E.; Meerhoff, M.; Moss, B.; Mulder, C.; Shurin, J. B.; Suttle, B.; Thompson, R.; Trimmer, M.; Woodward, G.; Guy, W.; Eoin, J. O. G. Mesocosm experiments as a tool for ecological climate change research. *Adv. Ecol. Res.* **2013**, *48*, 71–181.

- (24) Leuzinger, S.; Luo, Y.; Beier, C.; Dieleman, W.; Vicca, S.; Körner, C. Do global change experiments overestimate impacts on terrestrial ecosystems? *Trends Ecol. Evol.* **2011**, *26* (5), 236–241.
- (25) Singh, B. K.; Bardgett, R. D.; Smith, P.; Reay, D. S. Microorganisms and climate change: Terrestrial feedbacks and mitigation options. *Nat. Rev. Microbiol.* **2010**, *8* (11), 779–790.
- (26) Falkowski, P. G.; Oliver, M. J. Mix and match: How climate selects phytoplankton. *Nat. Rev. Microbiol.* **2007**, *5* (10), 813–819.
- (27) Srivastava, D. S.; Kolasa, J.; Bengtsson, J.; Gonzalez, A.; Lawler, S. P.; Miller, T. E.; Munguia, P.; Romanuk, T.; Schneider, D. C.; Trzcinski, M. K. Are natural microcosms useful model systems for ecology? *Trends Ecol. Evol.* **2004**, *19* (7), 379–384.
- (28) Vallino, J. J. Improving marine ecosystem models: Use of data assimilation and mesocosm experiments. *J. Mar. Res.* **2000**, *58* (1), 117–164.
- (29) Shaver, G. R.; Canadell, J.; Chapin, F. S.; Gurevitch, J.; Harte, J.; Henry, G.; Ineson, P.; Jonasson, S.; Melillo, J.; Pitelka, L.; Rustad, L. Global warming and terrestrial ecosystems: A conceptual framework for analysis. *Bioscience* **2000**, *50* (10), 871–882.
- (30) Wu, Z. T.; Dijkstra, P.; Koch, G. W.; Penuelas, J.; Hungate, B. A. Responses of terrestrial ecosystems to temperature and precipitation change: A meta-analysis of experimental manipulation. *Global Change Biol.* **2011**, *17* (2), 927–942.
- (31) Gao, K.; Helbling, E. W.; Häder, D. P.; Hutchins, D. A. Responses of marine primary producers to interactions between ocean acidification, solar radiation, and warming. *Mar. Ecol.: Prog. Ser.* **2012**, *470*, 167–189.
- (32) Harte, J.; Torn, M. S.; Chang, F. R.; Feifarek, B.; Kinzig, A. P.; Shaw, R.; Shen, K. Global warming and soil microclimate - Results from a meadow warming experiment. *Ecol. Appl.* **1995**, *5* (1), 132–150.
- (33) Conant, R. T.; Ryan, M. G.; Ågren, G. I.; Birge, H. E.; Davidson, E. A.; Eliasson, P. E.; Evans, S. E.; Frey, S. D.; Giardina, C. P.; Hopkins, F. M.; Hyvönen, R.; Kirschbaum, M. U. F.; Lavallee, J. M.; Leifeld, J.; Parton, W. J.; Megan Steinweg, J.; Wallenstein, M. D.; Martin Wetterstedt, J. Å.; Bradford, M. A. Temperature and soil organic matter decomposition rates – Synthesis of current knowledge and a way forward. *Global Change Biol.* **2011**, *17* (11), 3392–3404.
- (34) Hungate, B. A.; Dukes, J. S.; Shaw, M. R.; Luo, Y.; Field, C. B. Nitrogen and climate change. *Science* **2003**, *302* (5650), 1512–1513.